ACS chemical biology

ARTICLE

A LuxP-Based Fluorescent Sensor for Bacterial Autoinducer II

Jinge Zhu and Dehua Pei*

Department of Chemistry and Ohio State Biochemistry Program, The Ohio State University, 100 West 18th Avenue, Columbus, Ohio 43210

ABSTRACT Autoinducer 2 (AI-2), which enables different bacterial species to engage in interspecies communication, has been difficult to detect quantitatively. Currently, the most commonly used method for AI-2 detection employs an engineered *Vibrio harveyi* reporter strain, which produces bioluminescence in response to AI-2. However, the bioassay is not quantitative and is sensitive to assay conditions. In this work, we have developed two protein sensors for AI-2 by modifying AI-2 receptor proteins LuxP and LsrB with environmentally sensitive fluorescent dyes. The protein sensors bind specifically to AI-2 and produce dose-dependent changes in their fluorescence yield. The new assay method has been applied to monitor the enzymatic synthesis of AI-2 in real time and determine the extracellular and intracellular AI-2 concentrations in several bacterial culture fluids.

*Corresponding author, pei.3@osu.edu.

Received for review October 5, 2007 and accepted November 30, 2007.

Published online January 24, 2008

10.1021/cb7002048 CCC: $40.75

Quorum sensing (QS) is a type of bacterial cell-to-cell communication that coordinates gene expression in response to cell density (*1*). It appears to be a common feature of most bacteria and has been shown to regulate a variety of functions, including symbiosis, virulence, competence, motility, sporulation, mating, conjugation, antibiotic production, and biofilm formation (*2, 3*). QS is mediated through the production, release, and subsequent detection of small signaling molecules called autoinducers (AIs). There are at least two major types of QS. Type 1 QS is species-specific and each bacterium uses a unique AI-1 or a unique combination of AI-1's (generally oligopeptides for Gram-positive bacteria and acylhomoserine lactones for Gram-negative bacteria). Type 2 QS utilizes a common signaling molecule, AI-2, to facilitate interspecies communication. AI-2 is biosynthesized from *S*-adenosylhomocysteine (SAH) by the sequential action of nucleosidase Pfs and *S*-ribosylhomocysteinase (LuxS), which convert SAH into adenine, homocysteine, and 4,5-dihydroxy-2,3-pentanedione (DPD) (*4*). Under physiological conditions, DPD undergoes spontaneous cyclization to form various furanones as AI-2 or AI-2 precursors. In *Salmonella typhimurium*, the active form of AI-2 is thought to be (2*R*,4*S*)-2-methyl-2,3,3,4-tetrahydroxytetrahydrofuran (R-THMF), whereas a borate diester of (2*S*,4*S*)-2-methyl-2,3,3,4-tetrahydroxytetrahydrofuran (BAI-2) is the active AI-2 in *Vibrio harveyi* (*5, 6*).

In *V. harveyi*, detection of BAI-2 is mediated by LuxP, which belongs to a large family of bacterial periplasmic binding proteins (bPBPs) (*7*). The LuxP/BAI-2 complex interacts with LuxQ, a two-component sensory kinase/phosphatase (*8*). Sensory information from LuxPQ is transduced to a phosphotransferase protein LuxU. LuxU transmits the signal to a downstream response regula-

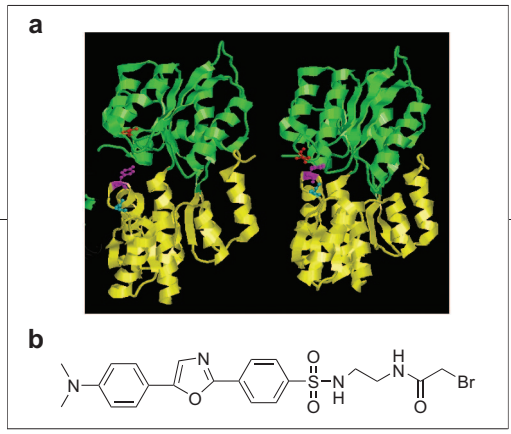

Figure 1. a) Comparison of apo- (left) and holo-LuxP (right) revealing the hinge-bending motion upon binding to BAI-2 (not shown). Residues mutated to cysteine are shown in red (Thr-137), cyan (Ser-207), and magenta (Tyr-210). b) Structure of fluorescent labeling reagent Dapoxyl.

tor LuxO, which turns on/off expression of the *luxCDABE* operon depending on its phosphorylation state. Like other bPBPs, LuxP consists of two domains linked by a hinge region, and the ligand-binding site is located at the interface between the two domains (Figure 1) (*6, 9*). In the apo form, LuxP exists in an open conformation with its ligand-binding site exposed to solvent. Upon binding to BAI-2, the two domains close up via a hinge-bending mechanism to completely engulf the ligand. In *S. typhimurium*, LsrB protein recognizes the R-THMF isomer and results in its uptake into the cytoplasm (*10*). LsrB is also a bPBP and is structurally similar to LuxP (*5*).

In light of the central role of AI-2 in QS-regulated biological processes, there is a need for a reliable, convenient method to monitor and quantify AI-2 levels in biological samples. Currently, the most commonly used method for AI-2 detection has been the bioassay developed by Bassler et al. (*11*), which utilizes a *V. harveyi* reporter strain (BB170) for bioluminescence induction. However, this bioassay is not quantitative (*12, 13*) and signal inhibition has been observed at high concentrations of AI-2 (*14–16*). It is also sensitive to assay conditions such as pH and the growth conditions of the reporter strain (*e.g.*, glucose levels) and susceptible to interference from indigenously produced AI-2 by the reporter strain (*12, 13, 17, 18*). Another method to detect AI-2 is to derivatize DPD with 1,2-phenylenediamine to form a stable quinoxaline derivative followed by HPLC analysis (*19, 20*). This method detects DPD in a sample instead of the active form of AI-2. It is also nonquantitative and time-consuming. Finally, we recently reported a FRET-based AI-2 assay, in which a cyan fluorescent protein (CFP) and a yellow fluorescent protein (YFP) were fused to the N- and C-termini of LuxP (*21*). Binding of BAI-2 to the chimeric protein causes a dose-dependent decrease in the FRET signal. This assay allowed us to determine the apparent dissociation constant (K_D) for BAI-2 and LuxP (*21*). Unfortunately, the overall FRET signal change between unbound and AI-2-bound states was very small, making this assay susceptible to interference from other species in a complex biological sample. In this study, we have developed two specific protein sensors for AI-2 by modifying LuxP and LsrB with environmentally sensitive fluorophores near their ligand-binding sites. The new assays are highly sensitive, fast responding, and relatively insensitive to interference. The AI-2 sensors have been applied to continuously monitor a LuxS-catalyzed reaction and quantify the extracellular and intracellular AI-2 levels of several bacterial culture fluids. The biochemical AI-2 sensors provide a useful alternative to the AI-2 bioassay and should find broad applications in QS-related studies.

RESULTS AND DISCUSSION

Construction and Characterization of AI-2 Sensors. Aided by the high-resolution structures of both free and AI-2-bound LuxP forms (Figure 1a) (*6, 9*), we selected three residues that are located at the rim of the AI-2-binding pocket, Thr-137, Ser-207, and Tyr-210, and individually mutated them into cysteines. Although the LuxP mutants also contain a cysteine at position 264, this cysteine is deeply buried in the structure and is not expected to react with any labeling reagent. Similarly, six LsrB mutants were generated by substitution of cysteine for Glu-67, Ser-69, Ser-94, Ser-117, Ser-161, or Tyr-194, on the basis of the crystal structure of a LsrB/AI-2 complex (*5*). To minimize labeling elsewhere on the protein, two surface cysteines on LsrB (Cys-99 and Cys-123) were replaced by serine in all of the above mutants. The LuxP and LsrB mutant proteins were each treated with eight different thiol-specific fluorescent labeling reagents including 6-acryloyl-2-dimethylaminonaphthalene (acrylodan), 6-bromoacetyl-2-(dimethylamino)naphthalene (badan), *N*,*N*′-didansyl-L-cystine (DDC), 5-((((2-iodoacetyl)amino)ethyl)amino)naphthalene-1-sulfonic acid (IAEDANS), 2-(4′-(iodoacetamido)-anilino)naphthalene-6-sulfonic acid (IAANS), 5-dimethylaminonaphthalene-1-sulfonyl (dansyl) aziridine, Dapoxyl (2-bromoacetamidoethyl)sulfonamide (Dapoxyl) (Figure 1b), and 1-(2-maleimidylethyl)-4-(5-(4-methoxyphenyl)oxazol-2-yl)pyridinium methanesulfonate (PyMPO), resulting in a total of 72 protein−dye pairs. These proteins were individually tested for AI-2 induced changes in fluorescent properties (Supplementary Fig-

TABLE 1. AI-2 induced changes in fluorescent properties of LuxP- and LsrB-based protein sensors

Protein	Fluorescent probe	Fluorescence change[a] (%)	Wavelength[a] (nm)	Shift in emission λ_{max} (nm)
LuxP-T137C[b]	Badan	28	494	0
LuxP-T137C	Acrylodan	20	488	−6
LuxP-S207C	Acrylodan	34	480	0
LuxP-Y210C	Acrylodan	79	466	−26
LuxP-S207C	DDC	35	496	0
LuxP-Y210C	DDC	66	498	0
LuxP-T137C	IAEDANS	−30	472	0
LuxP-T137C	IAANS	−29	452	−8
LuxP-S207C	Dansyl aziridine	44	498	0
LuxP-Y210C	Dansyl aziridine	96	496	0
LuxP-T137C	Dapoxyl	272	494	−41
LuxP-Y210C	Dapoxyl	41	499	−9
LsrB-S161C[c]	Dansyl aziridine	−14	495	0
LsrB-S69C	Dapoxyl	−4	496	0
LsrB-S94C	Dapoxyl	−7	497	0
LsrB-E67C	PyMPO	−4	552	0
LsrB-S161C	PyMPO	−7	550	0

[a]Values represent percentages of fluorescence signal changes at the specified wavelengths relative to those in the absence of AI-2. [b]For LuxP-based sensors, 14 μM BAI-2 was added to 5.6 μM fluorescently labeled LuxP mutants in 50 mM HEPES (pH 7.0) and 150 mM NaCl. [c]For LsrB-based sensors, 80 μM AI-2 was added to 8 μM fluorescently labeled LsrB mutants in 25 mM Tris (pH 8.0) and 150 mM NaCl.

ure S1). Among the 24 LuxP variants, 12 exhibited significant fluorescence changes upon BAI-2 binding (Table 1). Out of the 48 LsrB proteins, only five of them, dansyl-labeled S161C mutant (LsrB161Dan), Dapoxyl-labeled S69C (LsrB69Dap) and S94C mutants (LsrB94Dap), and PyMPO-labeled E67C (LsrB67Pym) and S161C mutants (LsrB161Pym), showed significant fluorescence changes with AI-2 binding (Table 1). Dapoxyl-labeled T137C mutant LuxP (LuxP137Dap) and LsrB161Dan were chosen for further studies due to their best overall properties (*e.g.*, large fluorescence change upon AI-2 binding, excellent labeling efficiency and specificity, and weak fluorescence of the underivatized labeling reagent).

When excited at 374 nm, LuxP137Dap exhibited moderate fluorescence emission with a maximum at 535 nm (Figure 2a). Upon the addition of saturating concentrations of BAI-2 (40 μM enzymatically synthesized DPD in the presence of 0.8 mM borate), an immediate increase in fluorescence yield was observed and the emission maximum blue-shifted to 494 nm. In contrast, LsrB161Dan showed strong fluorescence at 495 nm (with a shoulder at 520 nm) when excited at 340 nm, but its fluorescence yield decreased upon AI-2 binding (Figure 2b). Addition of 20 mM borate to the preformed LsrB/AI-2 complex did not perturb the fluorescence spectra (data not shown), consistent with the previous observation that LsrB recognizes a free furanone form of AI-2 (*5*). Incubation of the protein sensors with BAI-2 or AI-2 for 1 h at RT did not cause further changes in fluorescence (data not shown), indicating that the formation of LuxP/BAI-2 and LsrB/AI-2 complexes occurs rapidly and the complexes are stable. For both protein sensors, fluorescence changes are pH-dependent and optimal near physiological pH (Supplementary Figure S2). Note that the unconjugated Dapoxyl and dansyl aziridine have very weak fluorescence under the experimental conditions (Figure 2). Therefore, it is not necessary to remove the unreacted fluorescence probes after the protein labeling reaction.

To examine the specificity of the protein sensors, LuxP137Dap and LsrB161Dan were incubated with *S*-ribosylhomocysteine (SRH), LuxS enzyme, homocysteine, borate, and a variety of sugars and DPD analogues including D-ribose, D-xylose, L-arabinose, D-lyxose, D-xylulose, D-(+)-glucose, D-(−)-fructose, 1-(4-nitrophenyl)glycerol, 4-hydroxy-5-methyl-3(2*H*)-furanone, and dihydro-4,4-dimethyl-2,3-furandione (data not shown). Although LuxP and LsrB show strong structural homology to several sugar binding proteins, none of the above reagents induced significant fluorescence changes even at concentrations that are 10 times higher than the saturating AI-2 (or BAI-2) concentration. Thus, LuxP137Dap and LsrB161Dan are specific sensors for BAI-2 and AI-2, respectively.

Binding Affinity of LuxP and LsrB to AI-2. To determine the binding affinity of LuxP137Dap toward BAI-2, LuxP137Dap was incubated with varying concentrations of BAI-2 and the fluorescence spectra were recorded (Figure 2a). The fluorescence yield of the protein sensor increased with the BAI-2 concentration and eventually reached a maximum. Nonlinear regression fitting of the

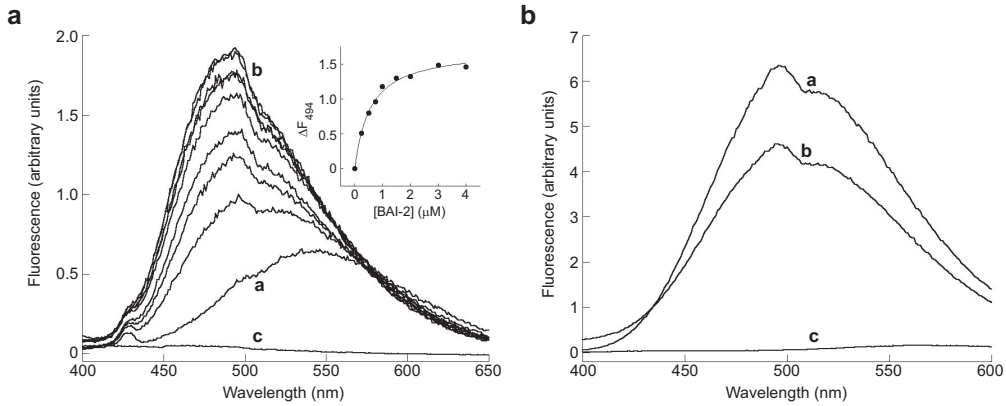

Figure 2. a) Effect of BAI-2 concentration (0, 0.25, 0.50, 0.75, 1.0, 1.5, 2.0, 3.0, 4.0 μM) on the fluorescence spectra (excitation at 374 nm) of LuxP137Dap (0.28 μM) in 50 mM HEPES (pH 7.0), 150 mM NaCl, and 0.8 mM borate: a, [BAI-2] = 0 μM; b, [BAI-2] = 4.0 μM; c, free Dapoxyl (8.4 μM). Inset, plot of LuxP137Dap fluorescence increase at 494 nm against BAI-2 concentration. The line was fitted to the data according to the equation $\Delta F = \Delta F_{max}[L]/([L] + K_D)$. b) Fluorescence spectra (excitation at 340 nm) of LsrB161Dan (11 μM) in the absence (a) and presence of 440 μM AI-2 (b) and free dansyl aziridine (c, 16.5 μM). The buffer contained 25 mM Tris (pH 8.0) and 150 mM NaCl.

fluorescence increase (ΔF) at 494 nm against BAI-2 concentration resulted in a dissociation constant (K_D) of 1.0 ± 0.4 μM (Figure 2a, inset). It should be pointed out that this K_D value is an apparent dissociation constant, since the actual BAI-2 concentration could not be accurately determined and was estimated to be 10% of the total DPD concentration (*22*). Similarly, an apparent K_D of 154 ± 34 μM was determined for the interaction between AI-2 and LsrB161Dan.

To confirm the results from fluorescence measurements, isothermal titration calorimetry (ITC) experiments were carried out to determine the binding affinity between AI-2 and the unmodified wild-type LuxP and LsrB. The ITC assay gave an apparent K_D value of 160 nM for the interaction between LuxP and BAI-2 (Supplementary Figure S3), in agreement with the previously measured K_D value (270 nM) from LuxP-FRET assay (*21*). It also indicates that the T137C mutation and/or derivatization by the Dapoxyl group resulted in a 6-fold reduction in binding affinity. To differentiate these two possibilities, the ITC experiments were repeated with unlabeled T137C LuxP protein and LuxP137Dap, and K_D values of 120 and 830 nM were obtained for T137C LuxP and LuxP137Dap, respectively. Therefore, the T137C mutation per se has essentially no effect on the binding affinity of LuxP. Rather, it is the addition of the large Dapoxyl group that interferes with BAI-2 binding, probably due to steric clashes. Similar ITC assay estimated a K_D value of ~160 μM for LsrB-AI-2 interaction.

Real-Time Monitoring of AI-2 Production. Previous LuxS activity assay monitors the release of homocysteine with 5,5′-dithiobis(2-nitrobenzoic acid) (DTNB) (*4, 19*). This assay suffers from several drawbacks such as high background signal due to DTNB hydrolysis and reaction with surface cysteines on LuxS as well as inactivation of LuxS by the DPD product. We have found that LuxP137Dap or LsrB161Dan may be directly added into a LuxS reaction to monitor the enzymatic production of DPD in real time. As shown in Figure 3a, when a LuxS reaction which contained 20 μM SRH, 11 μM LuxP137Dap, and 1.6 mM borate was initiated by the addition of 1 μM LuxS enzyme, the fluorescence yield increased essentially linearly with time (tracing a). The slight upward curvature is likely due to the fact that at the early stage the AI-2 concentration was very low and the binding between LuxP and BAI-2 was kinetically limited. When the amount of LuxS enzyme was doubled, the reaction rate was also approximately doubled (compare tracings a and b). In the absence of borate, no fluorescence change was observed; however, upon the addition of borate at 95 s, there was a sharp rise in fluorescence, followed by slower increase as a function of time (Figure 3a, tracing c). The abrupt fluorescence increase is due to rapid binding of AI-2 already accumulated in the solution to the protein sensor, whereas the

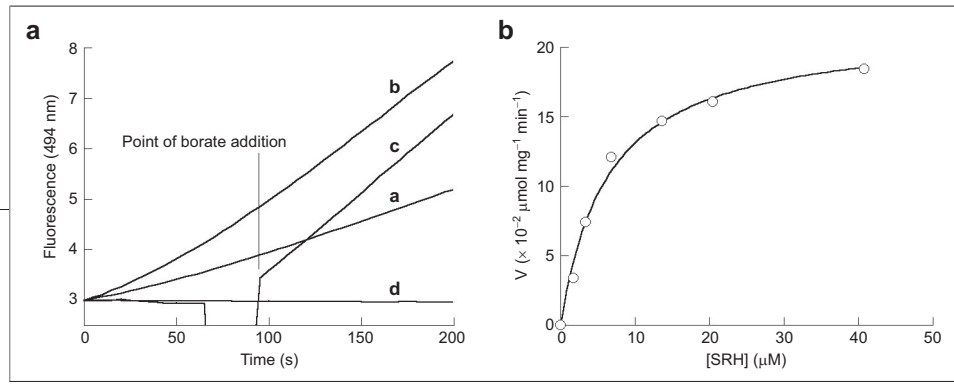

Figure 3. a) Reaction progress curves of Co-BsLuxS catalyzed conversion of SRH (20 μM) into DPD, as monitored with LuxP137Dap (11 μM) at 494 nm: a, [LuxS] = 1 μM; b, [LuxS] = 2 μM; c, [LuxS] = 2 μM, but borate was added 95 s after the addition of LuxS; d, control reaction without LuxS. The reaction buffer contained 50 mM HEPES (pH 7.0), 150 mM NaCl, and 1.6 mM borate. b) Michaelis–Menten plot of Co-BsLuxS activity as a function of SRH concentration.

slower phase represents the rate of enzymatic synthesis of AI-2. Note that the magnitude of the sharp rise was substantially lower than the corresponding value in the reaction that contained 1.6 mM borate (compare tracings b and c). This is likely due to inhibition of LuxS by the accumulated DPD; in the presence of borate, DPD was immediately converted into BAI-2 and became bound to LuxP137Dap (therefore less inhibition of LuxS). By using LuxP137Dap (11 μM) as the sensor and carrying out reactions at different SRH concentrations (0–60 μM), we were able to determine the kinetic constants of Co^{2+}-substituted *Bacillus subtilis* LuxS (Co-BsLuxS) as k_{cat} of 0.063 s^{-1}, K_M of 6.0 μM, and k_{cat}/K_M of 1.0×10^4 M^{-1} s^{-1} (Figure 3b). With LsrB161Dan as the sensor, the kinetic constants of *Escherichia coli* Co-LuxS (Co-EcLuxS) were obtained as k_{cat} of 0.45 s^{-1}, K_M of 14 μM, and k_{cat}/K_M of 3.2×10^4 M^{-1} s^{-1}. The k_{cat} and K_M values of Co-BsLuxS were ~2-fold higher than those determined with the DTNB assay (*19*), consistent with the notion that in the DTNB assay, the LuxS enzyme was partially inhibited by the DPD product. Another major advantage of the current assay is the absence of background fluorescence increase in the absence of LuxS reaction (Figure 3a, tracing d).

Quantification of AI-2 Concentration in Cell Culture. To test whether the protein sensors are capable of detecting AI-2 in complex mixtures, *E. coli* BL21(DE3) culture at the early stationary phase was centrifuged to remove the cells and the resulting cell-free medium was directly added to a LuxP137Dap solution. Addition of the cell-free medium alone resulted in significant increase in fluorescence intensity between 400 and 550 nm (10–20% increase at 494 nm) but not at wavelengths above 550 nm (Figure 4a). Since the same fluorescence increase was also observed with *E. coli* DH5α cells (Figure 4b), which carry a defective *luxS* gene, this increase must be due to the presence of other fluorescent species in the culture media (Supplementary Figure S4). Simultaneous addition of the BL21(DE3) medium and 1.6 mM borate resulted in a much larger increase in fluorescence intensity and a shift of emission maximum from 535 to 494 nm (Figure 4a). In contrast, addition of borate to the DH5α cell medium did not result in any further increase in fluorescence signal (Figure 4b). We attributed the fluorescence increase associated with borate addition to the formation of LuxP/BAI-2 complex and used this signal increase to quantitate AI-2 concentrations in the growth media.

E. coli [BL21(DE3) and DH5α], *Enterococcus faecalis*, *Staphylococcus epidermidis*, and *B. subtilis* cells grown in LB or minimal media were withdrawn from various time points of the growth curves and their cell-free media were assayed for AI-2 levels using LuxP137Dap as the reporter. The extracellular AI-2 concentration of BL21(DE3) cells was very low in the early lag phase but rapidly increased and reached the maximal level of 120 ± 20 μM during the late exponential phase and then gradually decreased as cells entered the stationary phase, eventually to below the detection limit of 1 μM (Figure 4c). The intracellular AI-2 concentration of BL21(DE3) cells was also measured by harvesting the cells by centrifugation and cell lysis by lysozyme treatment or passing through a French pressure cell (Supplementary Figure S5). The intracellular AI-2 levels followed essentially the same profile but had two distinctive features. First, the intracellular AI-2 concentration was much higher than the extracellular value, with a maximal level of 2 ± 0.2 mM (Figure 4c). Second, the intracellular AI-2 level peaked slightly earlier (by ~1 h) than the extracellular level did. As expected, no AI-2 could be detected from DH5α cells at any stage of cell growth (Figure 4c). The effect of growth conditions on AI-2 production was assessed by comparing the production of AI-2 from *E. coli* grown in LB vs minimal media. Similar extracellular AI-2 levels were observed in both media, but the intracellular AI-2 levels were ~2-fold higher in cells grown in minimal medium than in LB medium (Supplementary Figure S6). The Gram-positive bac-

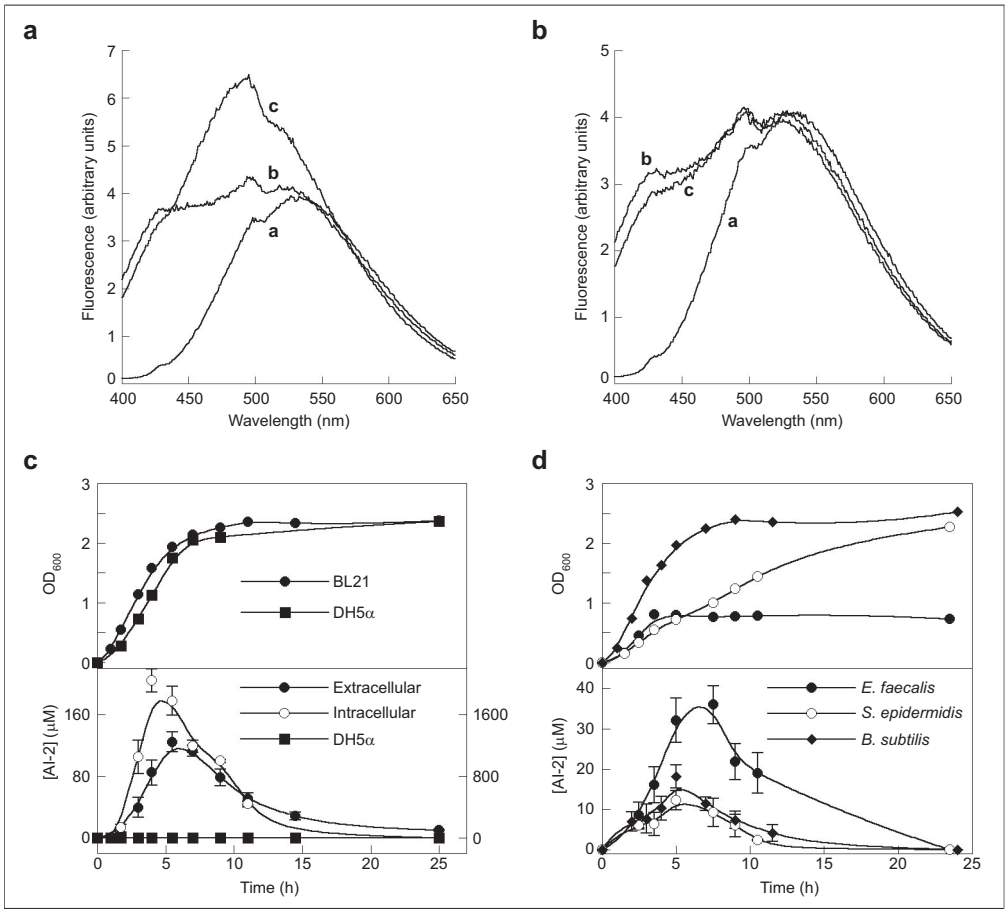

Figure 4. a) Fluorescence spectra of LuxP137Dap before and after addition of cell-free culture fluid of *E. coli* BL21(DE3) cells grown in LB medium to the late exponential phase (OD_{600} = 2.0): a, no cell culture fluid added; b, after addition of 7% (v/v) cell-free media; c, after addition of 7% cell-free media and 1.6 mM borate. Buffer: 50 mM HEPES (pH 7.0) and 150 mM NaCl. [LuxP] = 5.6 μM. b) Same as panel a except that the culture fluid of DH5α cells was used. c) Production of AI-2 by *E. coli* BL21(DE3) and DH5α cells in relation to cell growth: top panel, cell growth curve (as monitored by optical density at 600 nm); bottom panel, extracellular (*y* axis label on the left) and intracellular AI-2 concentrations (*y* axis label on the right) of BL21(DE3) cells. d) Production of AI-2 by *E. faecalis*, *S. epidermidis*, and *B. subtilis* cells in relation to cell growth: top panel, cell growth curve; bottom panel, extracellular AI-2 concentrations as a function of time. The error bars represent the standard deviations from three independent sets of experiments.

teria *E. faecalis*, *S. epidermidis*, and *B. subtilis* showed very similar extracellular AI-2 production profiles, except that their maximal AI-2 levels were 3.5-, 10-, and 7-fold lower than that of *E. coli* cells, respectively (Figure 4d).

Finally, as a comparison, we attempted to determine the extracellular and intracellular AI-2 concentrations of BL21(DE3) cells as a function of time by using our previously reported FRET assay (*21*). The extracellular AI-2 levels followed a similar trend to that in Figure 4, with a maximal value of 175 μM at the late exponential phase (Supplementary Figure S7). However, due to the narrow change in the FRET ratio (from 1.70 to 1.45), there were large fluctuations in the measured values. As a result, multiple measurements of serially diluted culture fluids (eight total) and data averaging were necessary to obtain a reliable value at each time point. Our attempts to quantify the intracellular AI-2 concentration by the FRET assay were unsuccessful.

Concluding Remarks. bPBPs are ideally suited for the development of reagentless biosensors. They exist in two drastically different conformations in the absence *vs* presence of ligands. Ligand binding induces a large, hinge-bending conformational change that alters the environment of the ligand-binding site. Over a dozen bPBPs have been modified with environmentally sensitive fluorophores to generate specific biosensors for diverse ligands including sugars, amino acids, anions, cations, and dipeptides (*23–25*). In this work, we have converted LuxP and LsrB into specific AI-2 biosensors. The LuxP-based biosensor has a similar sensitivity to the *V. harveyi* bioassay, with a detection limit of ~1 μM. However, our method is quantitative and can accurately determine AI-2 concentrations in complex mixtures such as bacterial culture fluids and crude cell lysates. With an apparent K_D of 1.0 μM between LuxP137Dap and BAI-2, the LuxP-based sensor should be able to quantitate AI-2 concentrations in the range of 1–20 μM. For higher concentration ranges (20–2000 μM), LsrB161Dan may be used (K_D = 154 μM for AI-2). Thus, the combination of LuxP- and LsrB-based biosensors provides a relatively broad dynamic range. Our assay is fast (<5 min) relative to the bioluminescence assay (3–6 h). Compared to the FRET assay we recently reported (*21*), the current assay is significantly more sensitive, due to a much larger fluorescent signal change upon ligand binding. Finally, our protein sensors are straightforward to prepare in any biochemical laboratory. Expression as a fusion protein with maltose binding protein (MBP) permits high yield (~100 mg per liter of culture) and facile purification. Subsequent incubation with 1.5 equiv of commercially available Dapoxyl (for LuxP) or dansyl aziridine (for LsrB) gives the desired protein biosensors, which can be used directly without further purification (the unlabeled dyes have negligible background fluorescence (Figure 2)). Note that LuxP and LsrB produced in DH5α cells (which carry a *luxS*$^-$ genotype) are in their apo forms.

By using the LuxP-based biosensor, we were able to determine both extracellular and intracellular AI-2 levels as a function of cell growth time. Our data indicate that both intracellular and extracellular AI-2 levels are low during the lag phase, increase rapidly during the logarithmic phase, reach the maximum during late logarithmic and early stationary phases, and then rapidly decrease as the cells enter the stationary phase (Figure 4). The qualitatively same profile has previously been generated by the bioluminescence assay (*26–31*). We found that the maximal AI-2 level (all DPD-derived species) reached 100–150 μM when *E. coli* cells were grown in rich media. The three Gram-positive bacteria had somewhat lower maximal AI-2 levels (12–36 μM). We have previously reported a BAI-2 concentration of 4.2 μM (corresponding to 42 μM AI-2) in the cell-free culture fluid of *V. harveyi* (*21*). Thus, all of the bacterial species that have been examined so far generally have a maximal extracellular AI-2 concentration of 12–150 μM. An interesting finding was that the intracellular AI-2 level is ~20-fold higher and peaks ~1 h earlier than the extracellular concentration. This suggests that AI-2 cannot freely diffuse across the cell membrane and may be actively exported by cellular machinery. The mechanism of AI-2 internalization during the stationary phase has recently been worked out in *E. coli* and *S. typhimurium* (*5, 10, 32, 33*). Given the apparent K_D of 0.2–0.3 μM for the LuxP/BAI-2 complex, these AI-2 levels are sufficient to bind to LuxP and turn on the signaling cascade.

In summary, the LuxP- and LsrB-based AI-2 biosensors permit sensitive, reliable, and quantitative detection of AI-2 in complex biological samples and are convenient to use. They provide a useful alternative to the conventional AI-2 bioluminescence assay and are likely to find widespread applications in the field of QS research.

METHODS

Materials. Fluorescent reagents (acrylodan, badan, IAEDANS, IAANS, dansyl aziridine, Dapoxyl, and PyMPO) were purchased from Molecular Probes (Eugene, OR). DDC was purchased from Sigma-Aldrich (St. Louis, MO). Oligonucleotides were from Invitrogen (Carlsbad, CA) and Integrated DNA Technologies (Coralville, IA). Restriction endonucleases, expression vector pMAL-c2x, and amylose resin were from New England Biolabs (Beverly, MA). All other chemicals and reagents were purchased from Sigma-Aldrich (St. Louis, MO) and Fisher Scientific (Pittsburgh, PA).

DNA Constructs. The gene encoding *V. harveyi* LuxP protein (*luxP*) was amplified from plasmid pGEX4T1-LuxP (kindly provided by Dr. Bonnie Bassler, Princeton University) by the polymerase chain reaction (PCR) using primers 5′-CGCGGATCCGTTTTGAATGGGTACTGG-3′ and 5′-ATGCGTCGACCTGCAGTCAATTATCTGAATATCTA-3′. The PCR product was digested with restriction endonucleases *Bam*HI and *Pst*I and subcloned into expression vector pMAL-c2x to generate plasmid pMAL-LuxP(ΔN23). In this construct, the first 23 amino acids of LuxP, which constitute the signal peptide, were removed and an MBP

was fused to its N-terminus. The gene coding for *S. typhimurium* LsrB protein (*lsrB*) was amplified from plasmid pQE30-CLBY (kindly provided by Dr. Richard Sayre, The Ohio State University) using primers 5′-CCGGAATTCGCAGAGCGGATTGCTTTTA-TTCCCAAACTG-3′ and 5′-GAATTCGGATCCTCAGAAATCATATTTGTCG-ATATTGTCTTT-3′ and cloned into *Eco*RI and *Bam*HI digested pMAL-c2x. The resulting construct, pMAL-LsrB(ΔN26), carried a deletion of the first 26 residues of LsrB and an N-terminal fusion with MBP. LuxP and LsrB mutants were generated in the above constructs using the QuikChange mutagenesis kit (Stratagene). The authenticity of each construct was confirmed by DNA sequencing.

Protein Expression and Purification. *E. coli* DH5α cells (3 L) carrying the proper plasmid DNA were grown in Luria–Bertani (LB) media supplemented with 2 g L^{-1} D-(+)-glucose and 75 mg L^{-1} ampicillin at 37 °C to an OD_{600} of 0.6–0.7. The cells were induced by the addition of 250 μM isopropyl β-D-thiogalactoside and grown at 30 °C for an additional 4.5 h. Cells were harvested by centrifugation and resuspended in 80 mL of a lysis buffer (25 mM Tris, pH 8.0, 150 mM NaCl, 0.5% (v/v) Triton X-100, 0.5% (w/v) protamine sulfate, 25 μg mL^{-1} trypsin inhibitor, and 150 μg mL^{-1} chicken egg white lysozyme). The cells were lysed by stirring at 4 °C for 30 min, followed by centrifugation at 15500 rpm (SS-34 rotor) for 20 min. The supernatant was loaded on an amylose resin column (2.5 × 6 cm) equilibrated in amylose binding buffer (25 mM Tris, pH 8.0, and 150 mM NaCl). The column was washed with 100 mL of the binding buffer, and the protein was eluted with 10 mM maltose in the same buffer. Fractions containing the desired protein (as analyzed by 12% SDS-PAGE) were combined and concentrated in an Amicon apparatus (Millipore), adjusted to 25% (v/v) glycerol, quickly frozen in dry ice−isopropanol, and stored at −80 °C. Protein concentration (typically 30–50 mg mL^{-1}) was determined by the Bradford method using bovine serum albumin as standard. Typical yield was ~100 mg of protein per liter of culture.

Protein Labeling. Fluorescent probes were dissolved in DMSO to make 15–25 mM stock solutions and mixed with LuxP or LsrB (280 μM) in 50 mM HEPES (pH 7.5) and 150 mM NaCl to give a probe/protein ratio of 1.5:1 (mol/mol). The reaction mixture was kept overnight in the dark at 4 °C or for 2 h at RT. Any unreacted labeling reagents were removed by passing the reaction mixture (0.5 mL) through a G-25 column (2.5 × 17 cm). Alternatively, the labeled protein was purified on an amylose column (2.5 × 6 cm). The purified proteins typically showed a single fluorescent band on SDS-PAGE gels with an apparent molecular weight of ~80 kDa. The stoichiometry of the labeling reaction was determined by measuring the protein concentration and the absorption of fluorophore at the appropriate wavelength. The molar absorptivities of the fluorophores were either from the Molecular Probes handbook or experimentally determined as follows: acrylodan, 1.1×10^4 M^{-1} cm^{-1} (360 nm); badan, 1.1×10^4 M^{-1} cm^{-1} (365 nm); DDC, 8.4×10^3 M^{-1} cm^{-1} (328 nm); IAEDANS, 5.7×10^3 M^{-1} cm^{-1} (336 nm); IAANS 2.7×10^4 M^{-1} cm^{-1} (326 nm); dansyl aziridine, 4.1×10^3 M^{-1} cm^{-1} (340 nm); Dapoxyl, 2.4×10^4 M^{-1} cm^{-1} (374 nm); and PyMPO, 3.4×10^4 M^{-1} cm^{-1} (415 nm). The dye-to-protein ratios were typically 1.2:1 (mol/mol) under these labeling conditions.

Fluorescence Spectroscopy. DPD was prepared enzymatically from SRH by LuxS reaction as described previously (*21*). The concentration of DPD was determined indirectly by measuring the amount of homocysteine released using DTNB. DPD prepared in this manner was stable for up to 10 days when stored at 4 °C. BAI-2 was prepared in a similar manner but in the presence of 4 equiv of borate. Its concentration was corrected by a factor of 0.1 based on ^{11}B NMR analysis (*22*). Fluorescently labeled LuxP and LsrB proteins were diluted into 50 mM HEPES (pH 7.0) and 150 mM NaCl, or 25 mM Tris (pH 8.0) and 150 mM NaCl, and fluorescence spectra were recorded on an Aminco-Bowman series 2 spectrometer (Thermo Fisher Scientific) at RT with excitation at the following wavelengths: 360 nm for acrylodan, 365 nm for badan, 330 nm for DDC, IAEDANS, and IAANS, 340 nm for dansyl aziridine, 374 nm for Dapoxyl, and 415 nm for PyMPO.

To determine the binding affinity of fluorescently labeled LuxP toward BAI-2, increasing concentrations of BAI-2 (0–4 μM) were added to a solution containing 50 mM HEPES (pH 7.0), 150 mM NaCl, 0.8 mM borate, and LuxP (0.28 μM) until there was no further change in the emission spectra. Fluorescence change at 494 nm was plotted against ligand concentration and fitted to the equation:

$$\Delta F = \Delta F_{max}[L]/([L] + K_D)$$

where ΔF and ΔF_{max} are experimental and maximal fluorescence changes, respectively, [L] is the ligand concentration, and K_D is the dissociation constant. The binding affinity of LuxP (5.6 μM) toward AI-2 analogues (0–200 μM) was determined in the same fashion. The binding affinity of LsrB (1.1 μM) for AI-2 (0–500 μM) and AI-2 analogues (up to 4 mM) was determined in a similar way except that the buffer contained 25 mM Tris (pH 8.0), 150 mM NaCl, and no borate and fluorescence change at 495 nm was plotted.

Isothermal Titration Calorimetry. ITC was performed on a MicroCal VP-ITC microcalorimeter (Northampton, MA) at 25 °C. A stock solution of BAI-2 (50 μM) in 50 mM HEPES (pH 7.5), 0.9 mM Tris, 9 mM NaH_2PO_4-Na_2HPO_4, 177 mM NaCl, and 1.6 mM borate was added sequentially in 2 or 5 μL aliquots into 1.455 mL of a LuxP solution (5.5 μM) in the same buffer at 240 s intervals for a total of 25 injections. Similarly, a solution of AI-2 (4 mM) was sequentially added into LsrB protein (5.5 μM) in the above buffer (but without borate) in 10–25 injections. In parallel experiments, BAI-2 and AI-2 were titrated into the buffer alone under the same conditions to obtain the heat of dilution. The heat of reaction per injection was determined by integration of the peak areas and fitted against the one-site binding model using Origin 7.0 software to obtain the binding constants.

LuxS Activity Assay. The LuxS reaction mixture (total reaction volume 500 μL) contained 50 mM HEPES (pH 7.0), 150 mM NaCl, 1.6 mM borate, 11 μM LuxP137Dap, and 0–60 μM SRH. The reaction was initiated by the addition of LuxS enzyme (0.5–2 μM final concentration) and monitored continuously at 494 nm on an Aminco-Bowman series 2 spectrometer (excitation at 374 nm) at RT. The initial rates were calculated from the early regions of the progress curves (30 s for Co-EcLuxS and 100 s for Co-BsLuxS) and fitted to the Michaelis–Menten equation

$$V = k_{cat}[E]_0[S]/(K_M + [S])$$

using KaleidaGraph 3.6 to obtain the k_{cat} and K_M values. In a parallel experiment, a standard line was generated under the same conditions with known concentrations of DPD to define the relationship between fluorescence yield and the DPD concentration. LsrB161Dan was also used to monitor the LuxS reaction in a similar manner, except that the reaction buffer contained no borate, and the excitation and emission wavelengths were 340 and 495 nm, respectively.

Measurement of Physiological AI-2 Signal. Bacterial overnight cultures grown in LB medium or minimal medium supplemented with 0.25% (w/v) D-(+)-glucose, 2 μg mL^{-1} thiamin, 1 μg mL^{-1} D-biotin, 0.1% (w/v) $(NH_4)_2SO_4$, and a metal salt mixture (0.5 mM $MgSO_4$, 0.5 μM H_3BO_3, 0.1 μM $MnCl_2$, 0.5 μM $CaCl_2$, 10 nM $CuSO_4$, 1 nM ammonium molybdate) were diluted 30-fold into fresh media and grown at 37 °C. At various time points, aliquots were withdrawn and the cell density was

determined by measuring the OD_{600}. To determine the extracellular AI-2 concentration, 20–50 μL of the culture was centrifuged in a microcentrifuge (14000 rpm for 2 min) to remove the cells and the cell-free medium was added to 5.6 μM LuxP137Dap in 50 mM HEPES (pH 7.0) and 150 mM NaCl, and fluorescence spectra were recorded before and after incubation with 1.6 mM borate. Incubation time varied from 5 min (*E. coli*) to 40 min (*B. subtilis*) depending on the bacterial species. The AI-2 concentration was calculated from the fluorescence increase at 494 nm using known concentrations of DPD as calibration standards. To determine the intracellular AI-2 concentration, cells from different points of the growth curve were harvested by centrifugation and washed three times with 50 mM NaH_2PO_4–Na_2HPO_4 (pH 7.5) and 50 mM NaCl, resuspended in the same buffer, and lysed by incubation with 10 mg mL^{-1} lysozyme for 30 min at RT or by passing through a French pressure cell at 1500–2000 psi. For lysis by lysozyme, 1.2 mL of the cell culture was used and resuspended in 180 μL of the above buffer. When the French press was employed, 150 mL of the cell culture was withdrawn and resuspended in 12.5 mL of buffer. The crude lysate was centrifuged at 14000–15000 rpm (microcentrifuge or SS-34 rotor), the clear supernatant was added to the LuxP137Dap solution, and the fluorescence yields were measured as described above. Intracellular AI-2 concentrations were calculated based on the reported intracellular volume of 1.0×10^{-15} L for a single *E. coli* cell (*34*) and the assumption that 0.1 OD_{600} in rich media corresponds to 1×10^8 cells mL^{-1} (*35*). Measurement of AI-2 concentration by LuxP-FRET assay was performed as described previously (*21*). Briefly, serial dilutions of cell-free culture fluid or cell lysate were added to 0.22 μM CFP-LuxP-YFP in 50 mM HEPES (pH 7.0), 150 mM NaCl, and 1.6 mM borate, and fluorescence spectra were recorded with excitation at 440 nm. The AI-2 concentration was calculated from FRET ratio (526 nm/482 nm) change using known concentrations of DPD as standard.

Acknowledgment: This work was supported by National Institutes of Health Grant AI62901.

Supporting Information Available: This information is free of charge *via* the Internet.

REFERENCES

1. Fuqua, W. C., Winans, S. C., and Greenberg, E. P. (1994) Quorum sensing in bacteria: The LuxR-LuxI family of cell density-responsive transcriptional regulators, *J. Bacteriol. 176*, 269–275.
2. Miller, M. B., and Bassler, B. L. (2001) Quorum sensing in bacteria, *Annu. Rev. Microbiol. 55*, 165–199.
3. Bassler, B. L. (2002) Small talk: Cell-to-cell communication in bacteria, *Cell 109*, 421–424.
4. Schauder, S., Shokat, K., Surette, M. G., and Bassler, B. L. (2001) The LuxS family of bacterial autoinducers: Biosynthesis of a novel quorum-sensing signal molecule, *Mol. Microbiol. 41*, 463–476.
5. Miller, S. T., Xavier, K. B., Campagna, S. R., Taga, M. E., Semmelhack, M. F., Bassler, B. L., and Hughson, F. M. (2004) Salmonella typhimurium recognizes a chemically distinct form of the bacterial quorum-sensing signal AI-2, *Mol. Cell 15*, 677–687.
6. Chen, X., Schauder, S., Potier, N., Van Dorsselaer, A., Pelczer, I., Bassler, B. L., and Hughson, F. M. (2002) Structural identification of a bacterial quorum-sensing signal containing boron, *Nature 415*, 545–549.
7. Tam, R., Jr (1993) Structural, functional, and evolutionary relationships among extracellular solute-binding receptors of bacteria, *Microbiol. Rev. 57*, 320–346.
8. Federle, M. J., and Bassler, B. L. (2003) Interspecies communication in bacteria, *J. Clin. Invest. 112*, 1291–1299.
9. Neiditch, M. B., Federle, M. J., Miller, S. T., Bassler, B. L., and Hughson, F. M. (2005) Regulation of LuxPQ receptor activity by the quorum-sensing signal autoinducer-2, *Mol. Cell 18*, 507–518.
10. Taga, M. E., Miller, S. T., and Bassler, B. L. (2003) Lsr-mediated transport and processing of AI-2 in *Salmonella typhimurium*, *Mol. Microbiol. 50*, 1411–1427.
11. Bassler, B. L., Wright, M., and Silverman, M. R. (1994) Multiple signalling systems controlling expression of luminescence in *Vibrio harveyi*: Sequence and function of genes encoding a second sensory pathway, *Mol. Microbiol. 13*, 273–286.
12. DeKeersmaecker, S. C., and Vanderleyden, J. (2003) Constraints on detection of autoinducer-2 (AI-2) signalling molecules using Vibrio harveyi as a reporter, *Microbiology 149*, 1953–1956.
13. Turovskiy, Y., and Chikindas, M. L. (2006) Autoinducer-2 bioassay is a qualitative, not quantitative method influenced by glucose, *J. Microbiol. Methods 66*, 497–503.
14. Winzer, K., Hardie, K. R., Burgess, N., Doherty, N., Kirke, D., Holden, M. T. G., Linforth, R., Cornell, K. A., Taylor, A. J., Hill, P. J., and Williams, P. (2002) LuxS: Its role in central metabolism and the in vitro synthesis of 4-hydroxy-5-methyl-3(2H)-furanone, *Microbiology 148*, 909–922.
15. Meijler, M. M., Hom, L. G., Kaufmann, G. F., McKenzie, K. M., Sun, C., Moss, J. A., Matsushita, M., and Janda, K. D. (2004) Synthesis and biological validation of a ubiquitous quorum-sensing molecule, *Angew. Chem., Int. Ed. 43*, 2106–2108.
16. De Keersmaecker, S. C., Varszegi, C., van Boxel, N., Habel, L. W., Metzger, K., Daniels, R., Marchal, K., De Vos, D., and Vanderleyden, J. (2005) Chemical synthesis of (*S*)-4,5-dihydroxy-2,3-pentanedione, a bacterial signal molecule precursor, and validation of its activity in Salmonella typhimurium, *J. Biol. Chem. 280*, 19563–19568.
17. Vilchez, R., Lemme, A., Thiel, V., Schulz, S., Sztajer, H., and Wagner-Döbler, I. (2007) Analyzing traces of autoinducer-2 requires standardization of the *Vibrio harveyi* bioassay, *Anal. Bioanal. Chem. 387*, 489–496.
18. Xavier, K. B., and Bassler, B. L. (2005) Interference with AI-2-mediated bacterial cell-cell communication, *Nature 437*, 750–753.
19. Zhu, J., Dizin, E., Hu, X., Wavreille, A.-S., Park, J., and Pei, D. (2003) S-Ribosylhomocysteinase (LuxS) is a mononuclear iron protein, *Biochemistry 42*, 4717–4726.
20. Nedvidek, W., Ledl, F., and Fischer, P. (1992) Detection of 5-hydroxymethyl-2-methyl-3(2H)-furanone and of a-dicarbonyl compounds in reaction mixtures of hexoses and pentoses with different amines, *Z. Lebensm.–Unters. –Forsch. 194*, 222–228.
21. Rajamani, S., Zhu, J., Pei, D., and Sayre, R. (2007) A LuxP-FRET-based reporter for the detection and quantification of AI-2 bacterial quorum-sensing signal compounds, *Biochemistry 46*, 3990–3997.
22. Semmelhack, M. F., Campagna, S. R., Federle, M. J., and Bassler, B. L. (2005) An expeditious synthesis of DPD and boron binding studies, *Org. Lett. 7*, 569–572.
23. Gilardi, G., Zhou, L. Q., Hibbert, L., and Cass, A. F. (1994) Engineering the maltose binding protein for reagentless fluorescence sensing, *Anal. Chem. 66*, 3840–3847.
24. Marvin, J. S., and Hellinga, H. W. (1998) Engineering biosensors by introducing fluorescent allosteric signal transducers: Construction of a novel glucose sensor, *J. Am. Chem. Soc. 120*, 7–11.
25. de Lorimier, R. M., Smith, J. J., Dwyer, M. A., Looger, L. L., Sali, K. M., Paavola, C. D., Rizk, S. S., Sadigov, S., Conard, D. W., Loew, L., and Hellinga, H. W. (2002) Construction of a fluorescent biosensor family, *Protein Sci. 11*, 2655–2675.
26. Surette, M. G., and Bassler, B. L. (1999) Regulation of autoinducer production in *Salmonella typhimurium*, *Mol. Microbiol. 31*, 585–595.
27. Ohtani, K., Hayashi, H., and Shimizu, T. (2002) The luxS gene is involved in cell-cell signalling for toxin production in *Clostridium perfringens*, *Mol. Microbiol. 44*, 171–179.

28. Surette, M. G., and Bassler, B. L. (1998) Quorum sensing in *Escherichia coli* and *Salmonella typhimurium*, *Proc. Natl. Acad. Sci. U.S.A. 95*, 7046–7050.
29. Kim, S. Y., Lee, S. E., Kim, Y. R., Kim, C. M., Ryu, P. Y., Choy, H. E., Chung, S. S., and Rhee, J. H. (2003) Regulation of *Vibrio vulnificus* virulence by the LuxS quorum-sensing system, *Mol. Microbiol. 48*, 1647–1664.
30. Babb, K., von Lackum, K., Wattier, R. L., Riley, S. P., and Stevenson, B. (2005) Synthesis of autoinducer 2 by the lyme disease spirochete, *Borrelia burgdorferi*, *J. Bacteriol. 187*, 3079–3087.
31. Hardie, K. R., Cooksley, C., Green, A. D., and Winzer, K. (2003) Autoinducer 2 activity in *Escherichia coli* culture supernatants can be actively reduced despite maintenance of an active synthase, LuxS, *Microbiology 149*, 715–728.
32. Taga, M. E., Semmelhack, J. L., and Bassler, B. L. (2001) The LuxS-dependent autoinducer AI-2 controls the expression of an ABC transporter that functions in AI-2 uptake in *Salmonella typhimurium*, *Mol. Microbiol. 42*, 777–793.
33. Li, J., Attila, C., Wang, L., Wood, T. K., Valdes, J. J., and Bentley, W. E. (2007) Quorum sensing in *Escherichia coli* Is signaled by AI-2/LsrR: Effects on small RNA and Biofilm architecture, *J. Bacteriol. 189*, 6011–6020.
34. CyberCell Database (CCDB) http://redpoll.pharmacy.ualberta.ca/CCDB/index.html.
35. Elbing, K., and Brent, R. (2003) In *Current Protocols in Molecular Biology* (Ausubel, F. M., Ed.) unit 1.2, John Wiley & Sons, New York.